Laser Radar Metrology Measurements through a Chamber Window of James Webb Space Telescope Alignment Fixtures during Cryogenic Testing

T. Hadjimichael[1], D. Kubalak[1], A. Slotwinski[2], P. Davila[1], B. Eegholm[3], W. Eichhorn[1], J. Hayden[3], E. Mentzell[1], R. Ohl[1], G. Scharfstein[4], R. Telfer[5]

[1]NASA Goddard Space Flight Center.
[2]Nikon Metrology Inc., [3]Sigma Space Corp.
[4] Flexure Engineering, LLC, [5] Orbital Sciences Corp.

Abstract:

NASA's James Webb Space Telescope (JWST), the scientific successor to the Hubble Space Telescope, will be the premier space science program for astrophysics in the coming decade. Testing of subsystems is currently underway. Metrology measurements of critical subsystems under vacuum and cryogenic conditions are needed to ensure proper operation. However, current non-contact, laser-based measurement systems cannot operate under these conditions. This paper presents the results of measuring through a vacuum chamber window using a Nikon Metrology (formerly Metris) Laser Radar.

The accuracy of laser metrology measurements depends upon knowing the parameters of the media through which the measurement beam travels. Under normal conditions, this means knowledge of the temperature, pressure and humidity of the air in the measurement volume. Typically, thermal gradients provide the most challenging aspect of achieving accurate measurements but this can be overcome with temperature sensors along the measurement path to provide an average effect. Often, however, there is a need to measure an object in an environment unsuitable for the measurement instrument, such as in an extreme temperature environment. In the past, windows have been used to protect the measuring device from the heat of the molten metal in a steel mill but, due to the relaxed accuracy requirements, a rigorous model of the effect of the window on the measurement was not done.

In the case of the James Web Space Telescope alignment fixturing, high accuracy measurements through a window must be made with the components at cryogenic temperatures in a vacuum. The ability to make accurate measurements through a window presents a challenge as there are a number of factors to considerer. In the case of the laser radar, the window will increase the time-of –flight of the laser beam causing a ranging error, and refract the direction of the beam causing angular positioning errors.

A model is being developed to compensate for these effects and for the fact that part of the measurement path is in vacuum. Parameters being considered include the window material, thickness and shape. In addition, differences in pressure, temperature, and humidity on each side of the window will cause slight atmospheric index changes and induce deformation and a refractive index gradient within the window. Also, since the window is a dispersive media, the effect of both phase and group indices have to be considered. Ambient measurements taken on a target-filled test piece showed good agreement with the model. Cryogenic/vacuum measurements include an array of targets matching the laser radar's capabilities: holes, tooling balls, and various scan areas. These measurements are taken at specific points throughout the cycle of the cryogenic experiment and matched to modeling. Those measurements points are: without the window in place, with window at ambient, with window at vacuum, and at cryogenic temperature. This paper discusses our findings to-date.

Introduction:

Calibration ground support equipment (GSE) for the Integrated Science Instrument Module (ISIM) and Optical telescope element SIMulator (OSIM) itself needs to be calibrated at or below 40K [1,2]. The GSE alignment target plates consist of large (~1m), metal and composite structures containing a host of optical and mechanical metrology targets that are used by various ambient and cryogenic metrology systems during ISIM and OSIM alignment and test [3,4]. The purpose of these fixtures is to align the telescope-like output of OSIM to the flight coordinate system of ISIM. The ambient placement of these targets is arbitrary, but their cryogenic locations and orientations must be known to a high accuracy with respect to the coordinate system. Therefore, these fixtures must be independently calibrated at the cryogenic operating temperature. This testing will occur in an environmental chamber where only non invasive instrumentation will be able to measure dimensional changes to the GSE during its cold cycling. The experiments described in this paper are used to determine if metrology of the various targets is feasible using the Nikon Metrology Laser Radar (LR) and to help build and verify a LR-though-a-window optical model that will be used to correct raw metrology. 6.35mm diameter through holes, 200um pinholes, tooling balls, retro-reflectors and flat mirror targets were used to facilitate the understanding of how the LR works under test chamber-like conditions.

Test Facility and Target Array:

The Goddard Space Flight Center (GSFC) vacuum test facility is a 12' x 14' vertical loading thermal vacuum test chamber. The facility can operate from -120°C to +110°C in GN_2 mode; the temperature can reach -180°C in LN_2 mode.[1] Vacuum is achieved with three cryogenic pumps. The chambers cold shroud is designed for liquid nitrogen flow and there is a 3 ft x 3 ft stable plate in the center of the floor of the chamber for hardware mounting. We have also incorporated a separate cold plate to which our hardware and cold straps are mounted. The chamber sits on a concrete slab one floor below the viewports. At the observation level the floor is simply diamond plate and not suitable for placement of metrology instrumentation. The chamber floor and the observation floor being separate, any metrology equipment observing the target array inside the chamber would also observe any movements between the decoupled bases of the floors. In order to overcome this obstacle an aluminum seat clamps the LR to a stiffening I-beam that is part of the outside chamber wall. This seat holds both the LR and a theodolite as a secondary reference. In order to determine the impact of possible vibrations attributable to this mount on a quiescent chamber, observations of various targets inside the chamber without any chamber pumps running showed a small but inconsequential increase in RMS repeatability of target positions.

[1] For the calibration of the JWST alignment fixtures, an additional liquid helium capability will be utilized in order to reach the ~40 K operating temperature.

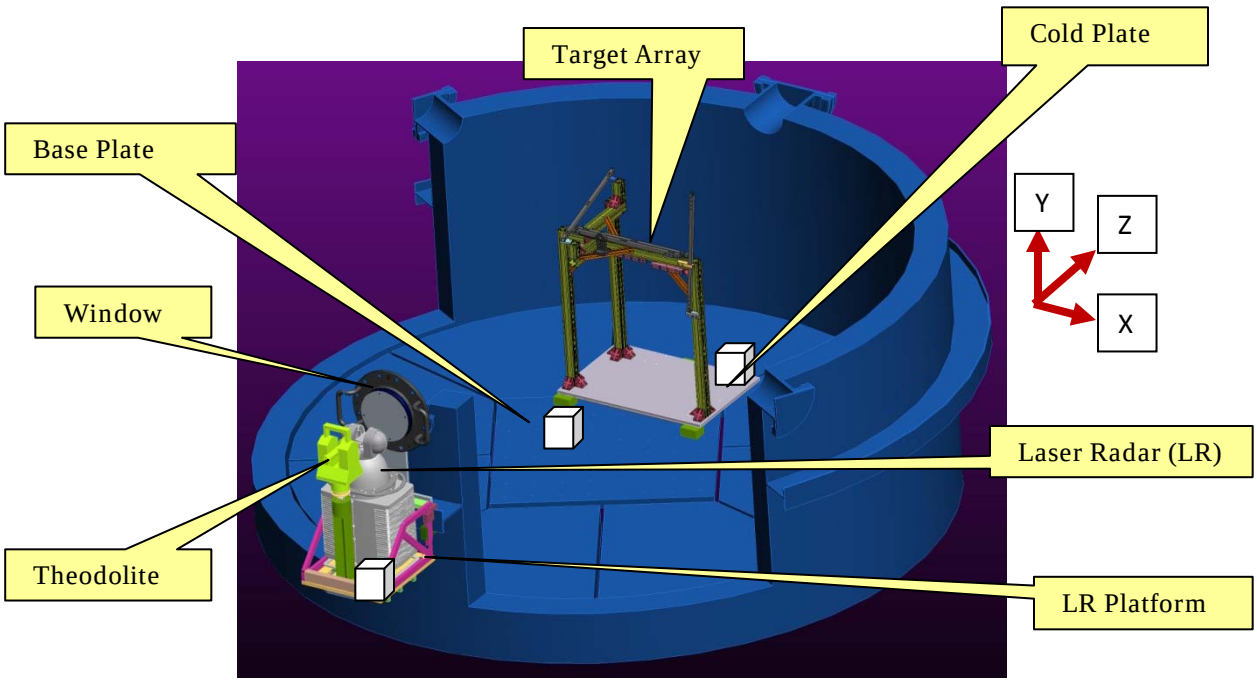

Figure 1: CAD image of vacuum chamber showing LR, theodolite and target array placement.

The target array was devised as a test platform for each of the different target types that the LR is required to measure during the calibration of the JWST GSE fixtures. The two main observation techniques we plan to utilize in the later GSE testing are the tooling ball and through hole measurement algorithms. Three aluminum scale bars were placed along three axes of the scene. The X and Y axis scale bars were approximately perpendicular to the LR path of light and Z parallel to it (range). Each of these ~730mm long scale bars accommodated a tooling ball at each end that was magnetically registered to the end of the bar. On one face of the Al scale bars, a 6.35mm through hole was drilled at the end of the bars near the tooling ball target. An additional Invar scale bar was added along the X axis and housed a tooling ball at either end. These scale bars allow for comparison between observed length changes warm-to-cold and calculated warm to cold length deltas in three dimensions. The scale bars were calibrated at GSFC during previous testing at ambient and cryogenic temperatures. Other targets on the test array include a standard flat 25.4mm diameter mirror, a 25.4mm diameter corner cube and two 200um pinholes. All data on these particular targets were observed with the different LR vision and metrology scanning techniques. In this paper, we limit our discussion to the hole and tooling ball targets on the scale bars.

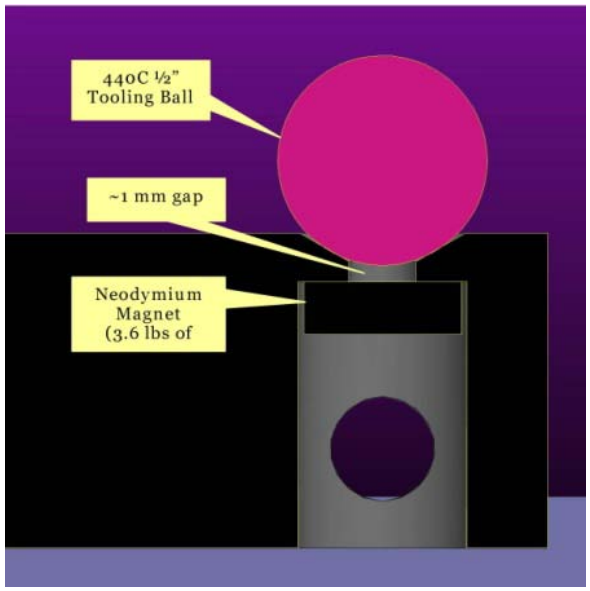

Figure 2: Drawing of tooling ball (pink) on end of a scale bar (black) being held by a magnet with through hole below.

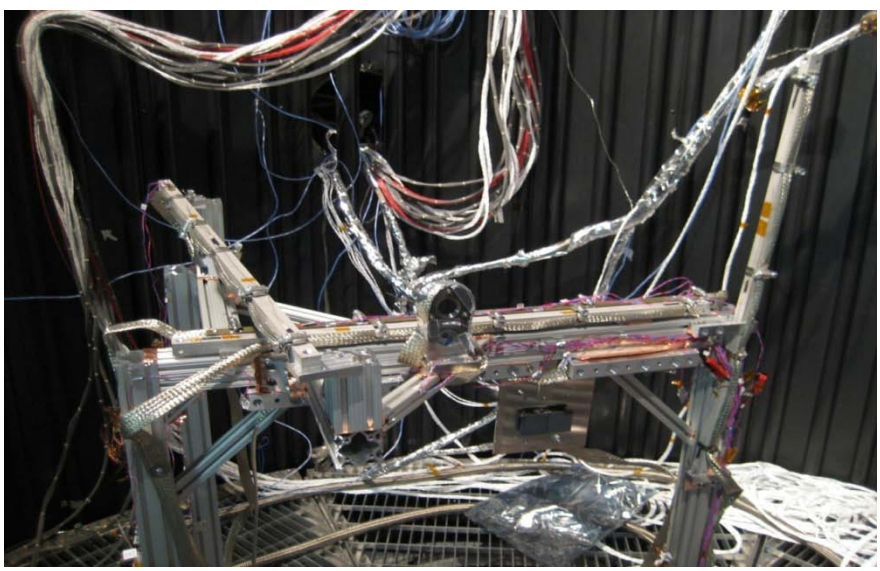

Figure 3: Photograph of target array showing X, Y, Z scale bars with holes and tooling balls

The chamber window (approximately 30.48 cm from the scanning mirror of the LR) is a 25.4 cm diameter Corning 7980 fused silica window with <1 arcsec wedge and flat to <λ/20 waves rms at λ =633nm total transmitted wavefront error over 60 % of the window diameter.[2,3] To acquire as much signal as possible from the LR (1550nm beam) both during transmission for the target array and in reflection to determine window placement no window coatings were added. In order to determine the index of refraction of the window (which is temperature dependant) during use, nine thermocouples were placed around the edges, four inside and four outside the chamber at ~90 degree intervals and one

[2] Corning, Inc., Corning, NY, www.corning.com
[3] Nu-Tek Precision Optical Corp., Aberdeen, MD, www.nu-tek-optics.com

on the inside window center. An outside thermocouple had been placed on the window center but it interfered with measurements later in the testing and was removed before cryogen was introduced into the system. Thermocouples were also placed at key positions inside the chamber (e.g., cold plate, etc.) and Platinum Resistance Thermometers (PRTs) were used on the aluminum scale bars for more accurate measurements. All targets were also strapped to the cold plate using tin-coated copper braid. Five Pipe clamps were used at equal intervals along the scalebars with PRTs to the cold strapping. All other targets were strapped to the cold plate to best effort via various fastening schemes. Given the limitations on test time and the LN2 capability of the cold plate, the targets reached temperatures 130 to140 K.

Testing:

Data were acquired during the following conditions: 1) All targets were measured without the window in place (i.e., the only media through which the LR signal passed was air). This case is considered the measurement baseline and all modeling-corrected results are compared to this case. 2) All targets were measured with the window in place, but under ambient pressure conditions. 3) The measurements were obtained with the window in place and the chamber at vacuum, but the test articles were at ambient temperature. 4) The test chamber was at vacuum and the test articles were cooled to ~140 Kelvin. All environmental data were tracked via thermocouples (or PRTs on scale bars) mounted throughout the test array and window, accelerometers on the stable plate and cold plate inside and the LR seat outside the chamber recorded vibrations, and chamber pressure was recorded by the facility personnel. The LR's external weather station recorded temperature, pressure and humidity for the short air path between the LR and the window. Each dataset consisted of measurements of all of the targets (holes, tooling balls, mirror, and retro-reflector) repeated five times for statistical purposes. As data were acquired, special attention was paid to repeatability. The repeatability for the ambient, no-window case in X, Y, Z positions was ~ 10-20um RMS, with the tooling balls repeating closer to ~10um and through holes to ~20um. Similar results were found with the window in place. However, after pulling vacuum, it was more difficult to get good repeatability through five datasets --- during the first cryo-cycle it was only possible to acquire data once all of the cryogenic pumps and vacuum pumps were turned off. Once all pumps were turned off, repeatability improved to ~15--30um RMS. Two full warm-to-cold cycles were accomplished in 8 days of testing.

Scale bars were placed approximately along the X (horizontal), Y (vertical), and Z (range) directions. Spatial Analyzer ™ software was used to determine lengths of the individual scale bars in each direction between targets (Table 1).[4]

LR MEASURED DATA (mm)							
Scale Bar	Length no window	L window Amb	DELTA	Amb/Vac	DELTA	Cryo	DELTA
X (holes)	729.848	734.865	5.016	734.4797	-0.385	732.1287	-2.351
Y (holes)	729.982	734.996	5.014	734.5847	-0.411	732.2277	-2.357
Z (TBs)	729.953	730.022	0.070	729.733	-0.289	727.4456	-2.288
X (TBs)	730.073	735.067	4.995	734.646	-0.422	732.3187	-2.327
INX (TBs)	730.222	735.129	4.907	734.850	-0.278	734.657	-0.193

Table 1: Laser Radar measured distances between targets on each scale bar. (No corrections for window or vacuum, only normal LR automatic environment corrections.)

[4] New River Kinematics, Inc., Williamsburg, VA, www.kinematics.com

The first column in Table 1 describes which scale bar was measured including which target. The next two columns are the lengths between targets as measured by the LR in Spatial Analyzer ™ the first without a window (baseline) and then with the window in place. The following column shows the differences between the two measurements. The last columns then show the measured lengths at vacuum and cryogenic temperature along with their respective differences from the window-in-place case. Note that the X and Y scale bars have very large deltas due to their positions with respect to the window normally corrected for through implementation of Snell's law. As light travels through the window and bends at the interface, large apparent deviations occur in where the LR system interprets target location. The data that are obtained approximately normal to the window serve as a convenient check on the data analysis process because the ray angle changes little and only range errors are realized between the "no window" and the "window" cases. The window's refractive index changes significantly as a function of wavelength. The Laser Radar, which uses an FMCW laser source at 1550nm, emits a chirped beam which is frequency swept about 100GHz. Light reflected off a target is recollected and coherently mixed with an optical local oscillator, or reference, signal to produce an RF signal proportional to the distance to the target. The Laser Radar's ranging function is calibrated in the factory against a HeNe interferometer. The pressure, temperature and humidity of the environment during factory calibration are recorded by the instrument and subsequent measurements are corrected when these environmental parameters change. Since air is not a significantly dispersive media (the difference in the phase and group indices at 1550nm is about 1ppm) this calibration method is sufficient for most applications.

The actual travel time of the Laser Radar's light depends upon the group velocity (or group index) of the medium through which it travels. However, the refraction angle depends upon the phase index. Therefore, for a dispersive media, the modeling has to use the group index to determine the travel time, or time of flight, of the measurement beam but must use the phase index and Snell's law to determine the diffraction angle.

Two different LR measurement algorithms were used: One for measuring the holes and one for the tooling balls. The "Hole" algorithm takes surface points along multiple bisected lines of a circle described by a center point and diameter input by the user (other user input parameters include chamfer size, # of points along a bisection and # of bisected lines). The algorithm then finds a measured center point of the hole from the surface plane and the circumference about which the measured signals drop-off. Tooling balls are measured by a spiral trace about a user-selected center to find the maximum return beam to the LR. Depending on the tooling ball size, an offset is also chosen to determine center as the LR only finds the surface normal and the range to the surface.

In order to measure window location, the "direct and through" algorithm is used. (The LR was too close to the window to scan it directly.) We placed a tooling ball such that it can be viewed by the LR both in virtual reflection off the window and as well as via direct line of sight. In this manner, the window-to-LR range and angular alignment (i.e. tip and tilt) can be derived. However we had to obtain a virtual image of the tooling ball in reflection for a window with no coating and, thus, little reflected light. This can be difficult. The solution was to lower the LR system's signal strength threshold for capturing a peak return from the tooling ball. Normally the amount of light returned to the LR is much brighter than other stray sources that can interfere with the LR capturing algorithm -- a peak threshold is set high in order to negate any spurious measurements. When making a direct and through measurement on an uncoated mirror like this window surface, dropping this threshold is dangerous and extra care needs to be taken in order to place the tooling ball such that any other return beams could not be mistaken for a tooling ball during the "through" portion of the measurement. During the "direct" portion this threshold was set back to the default value. [5]

[5] Spatial Analyzer User's Manual, New River Kinematics, Inc., v. 1.21.2008, p. 150—151

Model setup:

We have modeled the LR measurements through the window using FRED.[6] FRED is a flexible non-sequential ray trace software package that allowed us to define the coordinate system in the model to be identical to the coordinate system defined by the LR. We could then import the metrology data without coordinate system transformations.

The model is divided into three main regions as shown in Figure 4: the atmosphere outside the vacuum chamber, the window, and the atmosphere inside the vacuum chamber. The LR is located in the region outside the vacuum chamber. The LR measures the temperature, pressure and humidity in this region and assumes that the entire beam path has a uniform environment.

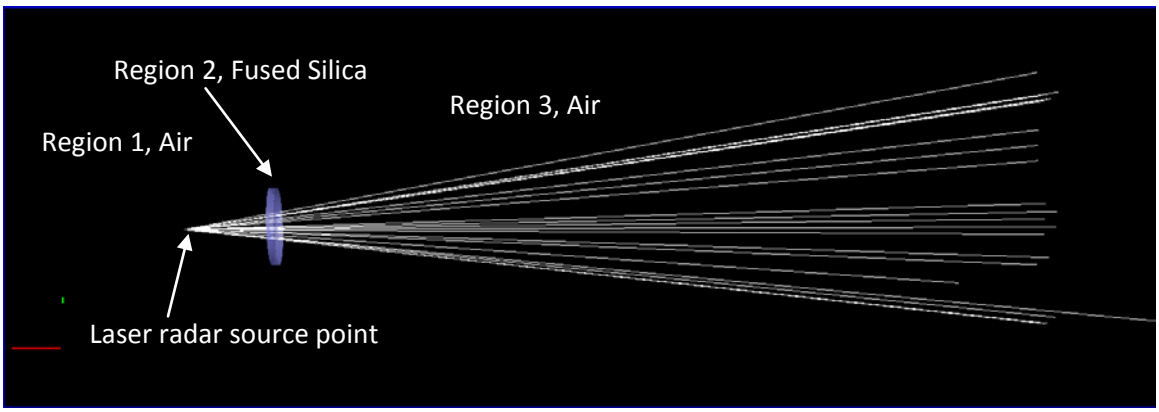

Figure 4: Schematic of the optical model of the LR measurements

The LR is modeled as a simple point source at the origin of the LR coordinate system. Light rays in the model are launched into directions defined by the final location reported by the LR measurements. For example, if a point as measured by the LR is at (x_o,y_0,z_0), then a ray is launched into space using $(x_0,y_0,z_0)/||(x_0,y_0,z_0)||$ as direction cosines. The distance the ray travels, as measured by the LR, is then $n_g||(x_o,y_0,z_0)||$, where n_g is the group index of refraction for air.

To calculate the group index of refraction for air, the Edlen equation was used [5,6,7]. The temperature, pressure, and relative humidity as reported by the LR were used to calculate the phase index of refraction, n_p, of air. The Edlen equation was programmed into the model using a user-scripted material. The group index, n_g, was then calculated by adding a small change, 0.001um, to the wavelength and using:

$$n_g = n_p - \lambda \frac{dn_p}{d\lambda}$$

where λ is the nominal LR test wavelength of 1.550um.

The window that was used is a fused silica window parallel to sub-arc second accuracy. The phase and group index for the glass were found as above, but with a temperature-dependent Sellmeier equation for fused silica. Temperature-depended Sellmeier coefficients for fused silica were calculated

[6] Photon Engineering, LLC, Tucson, AZ, www.photonengr.com

from measurements previously made by D. Leviton and B. Frey using the CHARMS system [8]. Again, a user-scripted material was used to implement this in the model.

The window alignment was determined using a “direct-and-through” measurement of the front surface of the window during each set of target measurements, as explained above. In this manner, the orientation of the window plane and distance from the LR to that plane are determined. The atmosphere inside the chamber was modeled using the same Edlen-defined air material outlined above for the atmosphere outside the chamber. For the vacuum cases, the path length in the chamber was modeled with an index of 1.0.

Ray tracing:

To model measurements made by the LR through the window, the ray tracing was handled in three parts. First, rays were traced into the directions as reported by the LR measurements, up to the first surface of the window. At that point, the optical path lengths as reported by FRED, which use the phase index, were corrected for group index. Next, the trace was done through the window to the second surface. Again, the optical path within the window was corrected for group index. Finally, the rays were propagated in space behind the window out to the distances reported by the LR measurements. The final modeled position, (x,y,z), was then reported and compared to measurements made by the LR without the window in place.

Results:

A target field consisting of fourteen (14) holes and seven (7) tooling balls on aluminum and Invar bars were measured with and without a window. Using the process outlined above, the with-window measurements were then run through the optical model to determine their true locations and compared against the no-window measurements. For the ambient case where the chamber vacuum pumps and cryogenic systems were not running, it was assumed that the targets and measurement system did not move between the measurements, so rigid-body motions have not been removed. The errors are shown below in Figure 5.

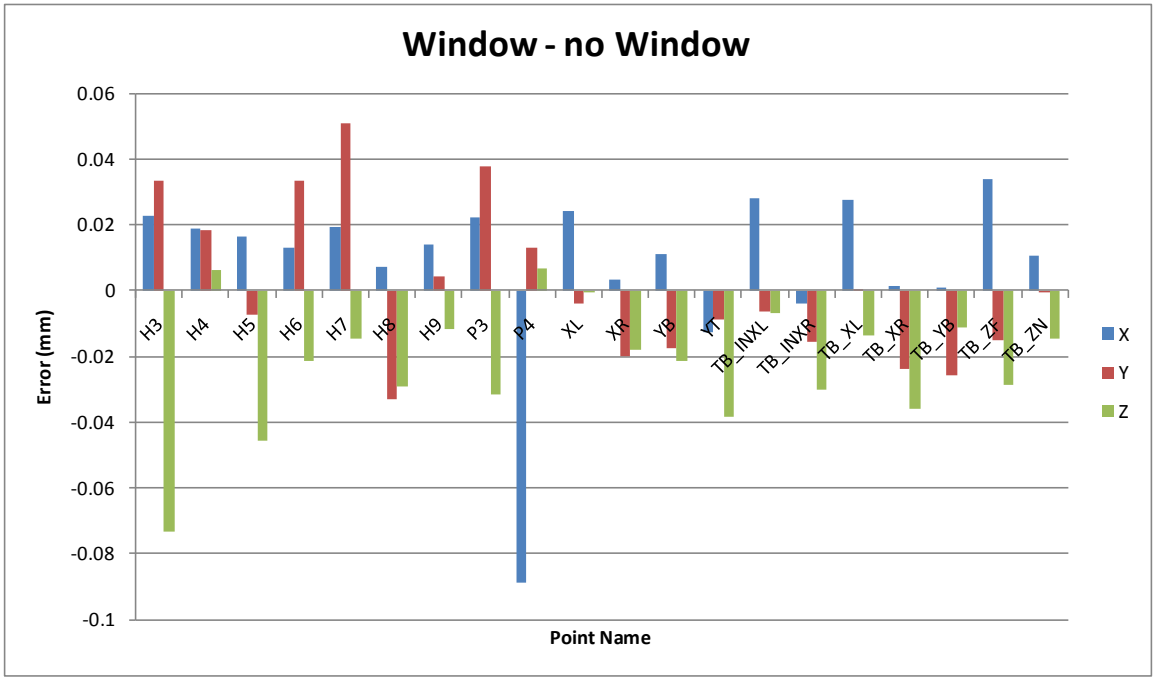

Figure 5: Errors between the modeled and measured locations of holes ('H' and 'P' points) and tooling balls ('TB' points).

The lengths of four scale bars were also calculated using the FRED optical model and compared with the lengths from the no-window measurements, using the CTE of the scale bars to predict warm-to-cold length change. Four scale bars were made of aluminum and one was Invar. There was a 1.2 K temperature drop recorded by temperature sensors on the rods between the two measurements, simply due to the temperature of the environment. By looking at the lengths of the scale bars, a relative measurement, rigid body alignment changes in the setup do not influence the result. The model and measurements agree to the values shown in Table 2.

Scale Bar	End points	Delta length change (mm)	material
X	(XL, XR)	0.0029	Aluminum
Y	(YL,YR)	0.0047	Aluminum
TB-INX	(TB-INXL, TB-INXR)	-0.0072	Invar
TB-X	(TB-XL, TB-XR)	-0.0042	Aluminum
TB-Z	(TB-ZL,TB-ZR)	-0.0016	Aluminum

Table 2: Differences between the lengths predicted by the FRED model vs. the length predicted from the no-window measurement taking into account temperature changes of the scale bars.

After the ambient window measurements were taken, the chamber was evacuated and the LR measurements were repeated. Following that, the chamber was taken down to LN2 temperatures and the LR measurements were again repeated. Temperature sensors on the scale bars reported temperatures around 140K. The vacuum window deformation was estimated using a NASTRAN analysis taking into account both the temperature and pressure effects. A polynomial fit of the window shape was calculated and entered into the model. Next the region inside the chamber was changed from air to vacuum.

The model was again used to predict the locations of the targets inside the chamber. These model-predicted locations were compared against the 'truth' values as measured by the LR without the window. Due to rigid body motions caused by chamber vibrations the errors for the ambient vacuum case were on the order of 1-1.5mm; for the cold measurements the errors were on the order of 2.5-3mm. For relative changes, however, we again compared the lengths of the scale bars as modeled against the predicted lengths calculated with the CTE's of the bars and the windowless measurements. The model and measurements agree to the values shown in Table 3.

Scale bar	End points	Ambient vac Delta length change (mm)	Cryo vac Delta length change (mm)	material
X	(XL, XR)	0.0140	0.0619	Aluminum
Y	(YL,YR)	0.0047	0.0033	Aluminum
TB-INX	(TB-INXL, TB-INXR)	-0.0103	-0.0021	Invar
TB-X	(TB-XL, TB-XR)	-0.0173	0.0283	Aluminum
TB-Z	(TB-ZL,TB-ZR)	0.0085	0.0115	Aluminum

Table 3: Differences between the lengths predicted by the FRED model vs. the length predicted from the no-window measurement taking into account temperature changes of the metering rods. These data are for a window with atmosphere on one side and vacuum on the other.

Summary:

The Laser Radar is a useful tool for taking metrology measurements without the need for physical interaction with the parts under test. In extreme cases when the parts are in extreme environments additional steps need to be taken to separate the operator and Laser Radar from that environment. In doing so the LR is unaware that the path of light is anything but the air in which its weather station resides. We have developed a model that accurately reduces the LR data and accounts for the three media in our testbed: air, fused silica and vacuum. This approach can be adapted for any environment/material. For our ~3m range setup, using group velocities to account for ranging errors and phase velocities for angular deviations through glass and air, the model solves for the absolute position of the measured points inside the environmental chamber to an average error (i.e. excursion) of ~11um at ambient temperature and ~21um for the cryogenic condition. These results support this technique for the cryogenic calibration of the JWST ISIM optomechanical alignment fixtures. These results are still in preliminary stages and my change slightly as further data reduction is conducted.

Acknowledgements:

This work was funded by the James Webb Space Telescope project at NASA Goddard Space Flight Center, Greenbelt, MD. The authors gratefully acknowledge support from S. Plander/Flexure LLC,

References:

[1] Greenhouse, Matthew A., et al., "The James Webb Space Telescope Integrated Science Instrument Module", Proceedings of the SPIE, Vol. 6265, p. 626513, 2006

[2] Davila, P., Bos., B., Cheng, E., Chang, B., Eichhorn, W., Frey, B., Garza, M., Gong, Q., Greeley, B., Guzek, J., Hakun, C., Hovmand, L., Kirk, J., Kubalak, D., Leviton, D., Nagle, A., Nyquist, R., Pham, T., Robinson, F. D., Sabatke, D., Sullivan, J., Volmer, P., von Handorf, R., and Youngworth, R., “Optical Telescope Element Simulator for the James Webb Space Telescope,” Proc. SPIE 7010, 70103F, 2008.

[3] Hagopian, J., Ohl, R., Bos, B., Davila, P., Eichhorn, W., Hylan, J., Hill, M., Nowak, M., Pasquale, B., Sampler, H., Wilson, M., Gallagher, B., Hardaway, J., Sullivan, J., Young, P., Keepers, T., and Quigley, R., “Optical alignment and test of the James Webb Space Telescope Integrated Science Instrument Module,” Integration, Alignment and Test of Large Optical Systems, IEE Aerospace Conf., 2007.

[4] Ohl, R., “Updates to the optical alignment and test plan for the James Webb Space Telescope integrated science instrument module,” Proc. SPIE 7433, 743305, 2009.

[5] Birch, K. P., and Downs, M. J., "An updated Edlén equation for the refractive index of air," Metrologia 30, 155-162 (1993)

[6] Birch, K. P., and Downs, M. J., "Correction to the updated Edlén equation for the refractive index of air," Metrologia 31, 315-316 (1994).

[7] Bonsch, G., and Potulski, E., "Measurement of the refractive index of air and comparison with modified Edlén's formulae," Metrologia 35, 133-139 (1998)

[8] Leviton, D. B., and Frey, B. J., “Cryogenic, High-Accuracy, Refraction Measuring System (CHARMS) – a new facility for cryogenic infrared through far-ultraviolet refractive index measurements,” SPIE, Glasgow, June, 2004